Study on flexural performance of prestressed glulam continuous beams under control influence

Lidan Mei[1], Nan Guo[1*] , Ling Li[1], Hongliang Zuo[1] and Yan Zhao[2]

Abstract

Traditional glulam beam connection mode has a weak ability to transfer bending moment, leading to insufficient joint stiffness and mostly in the form of simply supported beams. To make full use of material strength, a novel prestressed glulam continuous beam was proposed. On this basis, this paper put forward a new method to further improve the mechanical performance of the beams by controlling prestress. According to the estimated ultimate loads of the beams, six different control range values were formulated, and 12 continuous beams were tested for flexural performance. The effects of prestressing control on the failure modes, ultimate load capacity, and load versus deformation relationships of the glulam continuous beams were analyzed. The test results indicated that the flexural performance of the beams with prestressed control was significantly improved compared to the uncontrolled beams, the ultimate load was enhanced by 13.60%–45.11%, and the average steel wire stress at failure was increased from 70% of the designed tensile strength to 94%. Combined with the finite element analysis (FEA), the reasonable control range of the prestressed control continuous beams was18%–30% of the estimated ultimate load. The research in this paper can provide references for the theoretical analysis and engineering application of similar structures.

Keywords: Prestressed glulam continuous beams, Flexural performance, Experimental study, FEA, Control ranges

Introduction

Timber has significant advantages such as pollution-free, low energy consumption, and recyclability. Glulam is the most common engineering wood product in timber structure, reduces the impact of natural timber defects by processing natural timber, which can improve its strength and stiffness [1–9]. As one of the prominent flexural members in timber structure buildings, the glulam beam is of great significance to the safety of the whole structure. However, when the glulam beam was flexural, the tensile zone of the beam would be prone to brittle failure, and its compressive strength to be not fully used [10–15]. Furthermore, the length of the glulam beam does not

meet the requirements of the continuous beam due to the limit of raw material size and processing technology. And the current bolt connection has a weak ability to transfer bending moment, resulting in insufficient joint stiffness. Thus glulam beams are mostly simply supported beams [16–19]. To take full advantage of material properties and enrich structural forms, the author of this paper based on the previously proposed prestressed glulam simply supported beams, and then exploited the prestressed glulam continuous beam through a new set of connection apparatuses, as shown in Fig. 1a [20, 21]. The continuous beam combined two glulam beams through the new connection apparatus. In this case, the prestress can enhance the connection tightness between the two beams so this study regarded this connection method as a rigid connection realized by the apparatus and prestress. This paper aims to solve the problem that the application of prestressing is limited by the tensile strength of the top

*Correspondence: snowguonan@163.com
[1] College of Civil Engineering, Northeast Forestry University, Harbin 150040, China
Full list of author information is available at the end of the article
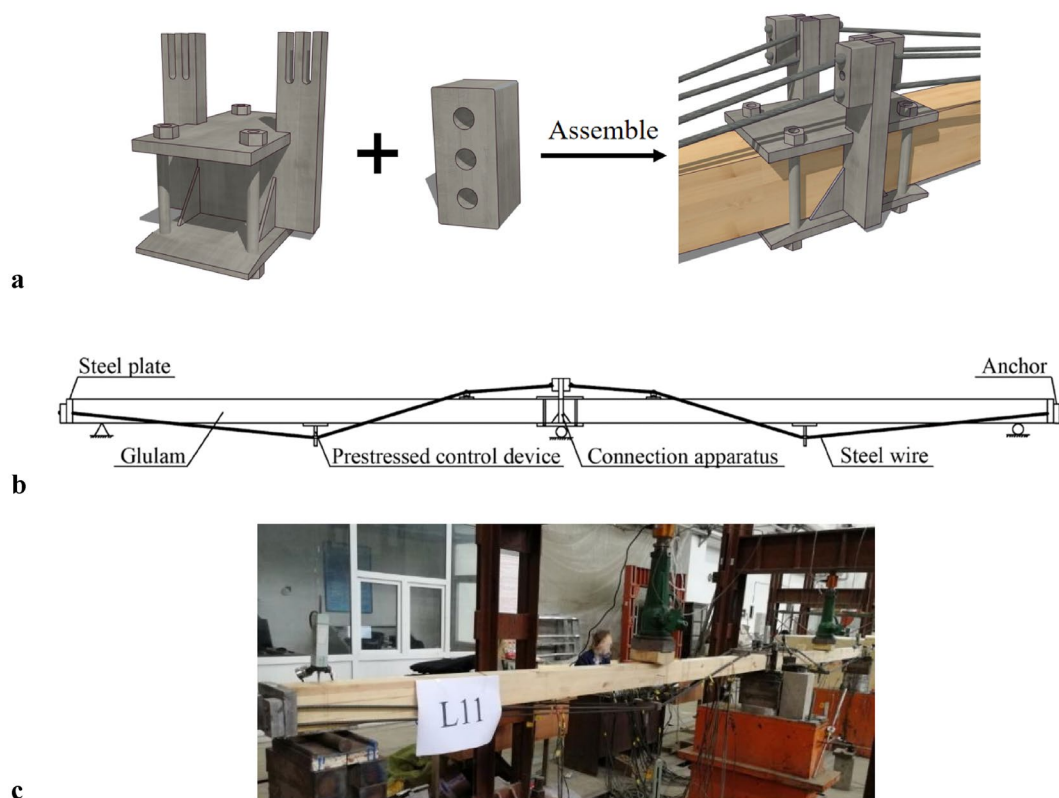
Fig. 1 Prestressed glulam continuous beam. **a** Details of connection apparatus; **b** details of the specimen; **c** photo of the specimen

of glulam beams. Thus, a new concept of prestressing control is proposed, namely, the beam is applied a certain range of load before prestressing, and then adjust the deflection of the beam to the state of the load is not applied. That is of great academic value and engineering significance to study the influence of the control range on the flexural performance of the prestressed glulam continuous beams.

More recently, some researchers have studied the combination of different materials and glulam to improve its strength. Uzel et al. [22] studied the flexural behaviors of glulam beams retrofitted with aluminum, fiberglass, and steel wire nets at the lamination surfaces. It was found that steel wire reinforcement nets can significantly increase the ultimate load-bearing capacity. Ribeiro et al. [23] proposed a concept of laminated wood composite with fiberglass and demonstrated the beneficial effect of the proposed strengthening solutions in terms of resistance and ductility. Zuo et al. [24] compared experiments on glulam beams reinforced by tapping screws. The results confirmed the importance of the reinforcements in enhancing ultimate load and stiffness. Yang et al. [25] proposed the reinforcement method of pasting steel plates or adding screws at the bottom of the glulam

beam. Results showed that the bending performance of glulam beams was improved.

To effectively enhance the flexural behavior of glulam beams and use the advantages of various materials, researchers applied the methods for strengthening glulam beams with prestressed materials. Anshari et al. [26] tested glulam beams were strengthened by inserting compressed wood blocks into the pre-cut rectangular holes from the top of the beam. Based on the moisture-dependent swelling nature of the compressed wood, a pre-camber was produced in the mid-span of the beam. A comparison with the beam without prestressing indicated that the initial stiffness and load-carrying capacity of the pre-stressed beam were increased significantly. Yang et al. [27] examined the reinforcing in flexure of glulam beams using bonded-in carbon fiber reinforced polymer bars. They found that the flexural capacity of prestressed and reinforced (bottom prestressed and top reinforced) beams increased up to 131%. McConnell et al. [28] conducted a series of four-point bending tests under post-tensioned glulam beams and indicated the flexural strength and stiffness increased for post-tensioned timbers. Previous studies have provided references for this paper from the use of different materials, prestressing

Mei *et al. J Wood Sci*   (2021) 67:48

Page 3 of 14

methods, and key factors affecting the mechanical performance of prestressed glulam beams.

This paper will examine the flexural behavior of 12 prestressed glulam continuous beams by considering the effect of control ranges. Failure modes, ultimate load capacity, and load versus deformation relationships will be investigated. And finite element analysis (FEA) will be conducted to obtain the optimally control range.

Materials and methods

Specimens and materials

In this paper, the prestressed glulam continuous beam was composed of glulam, high-strength steel wires, and steel components (Fig. 1). The steel components were comprised of connection apparatuses, prestressed control devices, steel plates, and anchors. The glulam with dimensions 3070 mm (length, L) × 80 mm (breadth, b) × 100 mm (height, h) was glued by five layers of 20 mm thick spruce planks. All specimens were set with four low-relaxation prestressed steel wires, which 12.9 mm in diameter.

Based on the previous work [29], the service load of the beam was about 30% of its ultimate load. Therefore, according to the previous research results and theoretical analysis, the ultimate load of the test beam was estimated during the research. Then, five control values were selected near 30% of the estimated ultimate load to explore the influence of different prestressed control

ranges on the flexural performance of the beams. Overall, six groups and 12 specimens were manufactured and tested. The groups and information of specimens are represented in Table 1.

All material properties were tested following the Chinese Standard GB/T50329-2012 [30] and GBT228.1-2010 [31]. The detailed mechanical properties of specimens as shown in Table 2.

Assembly procedure

As shown in Fig. 2, the assembly process of specimens included five steps: (1) the positioning lines of steel components and joints were drawn on the glulam beams; (2) prestressed control devices were attached to the corresponding positioning lines by adhesives, which were set for a while until the adhesive was completely solidified; (3) steel wires were cut and prepared in the length of design requirements, passed through anchors, and the ends of the steel wires anchoring by a machine; (4) after the glulam beams were jointed by connection apparatuses, the anchors at the ends of the steel wires were put into the slot of steel plates at the beam ends, and the steel wires were put into the prestressed control devices; (5) the initial load was applied to the beams by jacks, nuts in the prestressed control devices were tightened. Meanwhile, the jacks were unloaded to control the initial load within 1kN, and the deflection change was measured by the linear variable differential transformers (LVDTs) in the mid-span. When the reading values of LVDTs were not zero, which indicated that the length of the steel wires did not reach the required standard, it was necessary to add the plates between the anchors and the steel plates or cut the steel wires again.

Measurement layout

To measure the strain state of the glulam and the steel wires, the 100 mm × 3 mm strain gauges were pasted at the beam top, bottom and side of the mid-span. Since ribbed steel wires were used in this test, the steel wire surfaces at $L/4$ distance from the beams' support points were polished by an angle grinder, so it was convenient
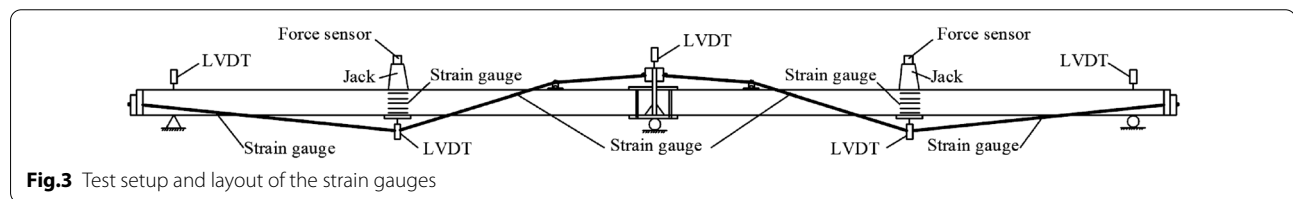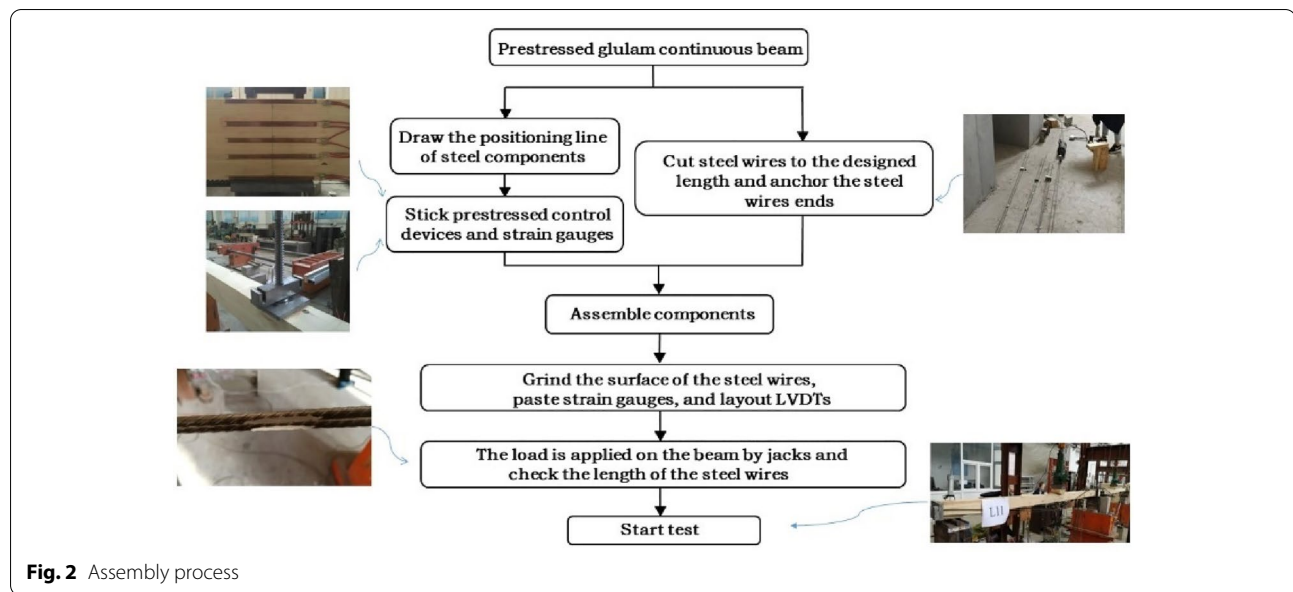
Table 1 Groups and information of specimens

Group	Beam code	Control range (%)[a]
1	L01, L02	0
2	L11, L12	18
3	L21, L22	24
4	L31, L32	30
5	L41, L42	36
6	L51, L52	42

[a] The percentage of the initial load to the estimated ultimate load of the beam

Table 2 Material properties

Material	Category	Average (N/mm²)	CoV (%)[a]
Spruce	Compression strength parallel to grain	38.67	6.151
	Modulus of elasticity in compression compression	8.301×10^3	4.630
	Tensile strength parallel to grain	81.32	6.184
	Modulus of elasticity in tensile	9.750×10^3	6.420
Steel wire	Tensile strength	1.640×10^3	0.3541
	Modulus of elasticity	1.920×10^5	1.710

[a] Coefficient of variation

Mei *et al. J Wood Sci*   (2021) 67:48

Page 4 of 14

Fig. 2 Assembly process

Fig.3 Test setup and layout of the strain gauges

Fig. 4 Static strain acquisition system

to paste the 2 mm × 3 mm strain gauges. To monitor the deflection of the beams, three LVDTs with a range of 50 mm were placed at its support, and an LVDT with a range of 150 mm was set in the mid-span (Fig. 3). JM3813 static strain acquisition systems (Yangzhou Jingming Technology Co., Ltd, China) were applied to collect the strain and deflection measurements, as shown in Fig. 4.

Loading mechanism

1. Preliminary load. According to the previous test results and theoretical analysis, the estimated ultimate load of the specimens was determined to be 30 kN. The pre-loading with 6%–12%–6% of the estimated ultimate load as a loading cycle, there were five cycles in total, and finally was restored to 0%. The experimental data did not include the above work results. The purpose of pre-loading is to eliminate the initial gaps between the components of the prestressed continuous beams.

2. Control of prestressing. The initial load (F) to be applied is 0%, 18%, 24%, 30%, 36% and 42% of the estimated ultimate load. The specimens generated deflection after the initial load was applied. After that, some researchers adjusted the deflection of the beam by twisting the prestressed control devices at the beam bottom and generated upward forces (F') to increase the pressure at the top of the beam. And then other researchers needed to unload the jacks simultaneously. In this process, the pressure sensor and DH3818 static strain acquisition system (Yangzhou Jingming Technology Co., Ltd, China) were

Mei *et al. J Wood Sci*   (2021) 67:48

Page 5 of 14

used to monitor the internal force changes, and the changes were controlled within 1kN. The prestressed control process is shown in Fig. 5.

3. Failure loading. The loading process started from the control range value, and the load increment of each level was 6% of the estimated ultimate load. When the loading reached 72% of the estimated ultimate load, the displacement control loading was used. In the stage of displacement control loading, the average value of the beam deflection increment under four levels of load between 48 and 72% of the estimated ultimate load was calculated. And this average value was taken as the displacement increment of each level of this stage until the beam failed.

Principles for determining failure and ultimate loads

According to the failure determination of wood components based on the Chinese Standard GB/T50329-2012 [30], as well as the failure determination of the reinforced concrete elements based on the Chinese Standard GB/T50152-2012 [32], and combined with the actual situation of this test, the failure signs of the glulam beams can be summarized as the following three situations. When one of them appears in the trial, it can be determined that the beam failed:

1. The tensile strain of the prestressed steel wire reaches 0.01.
2. Apparent cracks appear in the tension zone of the glulam beam, or significant wrinkles occur in the compression zone of the glulam beam. Also, the load–deflection curve decreases with loading.
3. The prestressed steel wire is broken, or the anchor device at the beam-end fails.

In the step loading test, the measured values of the ultimate load are determined according to the following principles:

1. When a failure sign appears during the loading process, the load value of the previous grade is taken as the measured value of the ultimate load in the test.
2. When the failure sign appears during the sustained loading process, the average value of the load of this grade and the load of the previous stage are taken as the measured value of the ultimate load in the test.
3. When the failure sign appears after the sustained loading is completed, the load value of this grade is taken as the measured value of the ultimate load in the test.
4. When the load–deflection curve decreases with loading, the peak point of the curve is used as the measured value of the ultimate load in the test.
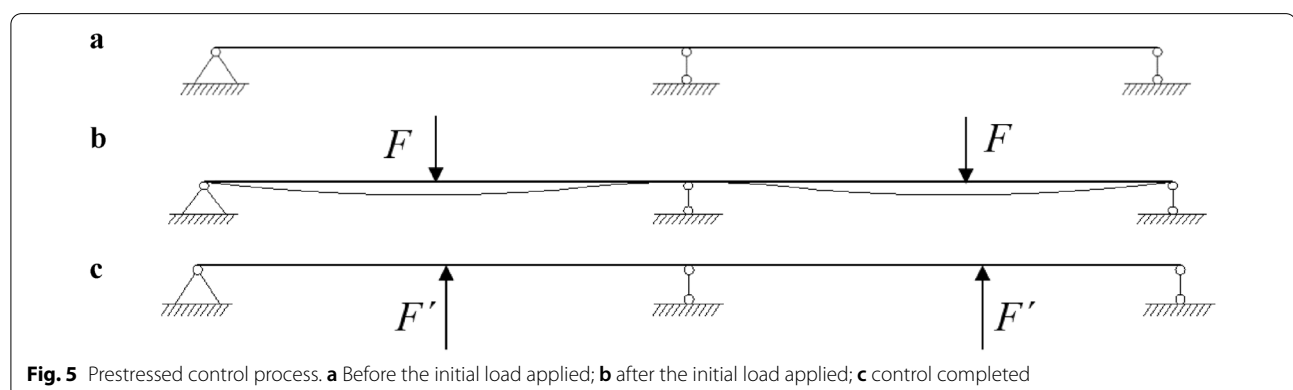
Experimental results and discussion
Failure modes
For all the specimens, the experimental phenomena can be classified into three main failure modes: compression failure at the beam top, tension failure of the weak areas between laminates, and instability failure. The specific contents are shown as follows:

1. Compression failure at the beam top
As the load increased, the deflection of the specimens increased gradually. When the load reached 90%–95% of the beams' ultimate load, wood knots or weak areas on the top of the beams appeared wrinkles because the glulam reached the compressive strength. With the continuous application of the load, the load no longer increased and showed a downward trend, each wrinkle began to extend and developed gradually. Finally, the beams were snapped off due to the tearing of the laminate at the

Fig. 5 Prestressed control process. **a** Before the initial load applied; **b** after the initial load applied; **c** control completed

Mei *et al. J Wood Sci*   (2021) 67:48

Page 6 of 14

wrinkles, and the beams were damaged. The typical failure modes of the specimens are shown in Fig. 6.

2. Tension failure of the weak areas between laminates
At the initial stage of loading, the deflection raised with the increase of load, and there was no apparent damage to the specimens. When the loading value reached 83%–89% of the peak load of the beams, the laminates were subjected to compression parallel to grain, which product tensile stress perpendicular to grain, and finally the tensile strength was insufficient. The longitudinal cracks first appeared at the weak areas of the laminates. They continued to extend to the beam ends, which significantly increased the deflection of the beams and reduced the load, and finally led to the decrease of the bearing capacity of the beams or the failure to continue loading, as shown in Fig. 7.

3. Instability failure
At the initial stage of loading, the deflection continued to increase, and there was no apparent damage to the beams. When the load was close to the peak load of the beams, bolt bars in the prestressed control devices gradually deflected out of the plane, which was due to the error in the cutting length of the steel wires, resulting in force distribution on the steel wires unevenly. Or because of the defects in the contact part of the glulam and steel plates along the beam width direction, it was not enough to uniformly resist the pressure exerted on the glulam by the bolt bars. When the glulam was damaged by local compression, the bolt bars would be deflected out of the plane. With the continuous loading, the load showed a downward trend, the fracture occurred at the weak areas of the laminate, and longitudinal tear occurred. Then the beams were broken at the loading position, and the beams were overturned as a whole, as shown in Fig. 8.

When the continuous beam was damaged, only one span was fully damaged, and the other span was not completely damaged or had no sign of fail. The incomplete damaged span was not representative, so only the failure mode of the completely damaged span was counted, as shown in Table 3.

Figure 9 presents the distribution of failure modes for all specimens. When the control range was small, the tensile stress of the steel wires was low. Compared with the stress produced by the compression at the beam end, the stress caused by the bending moment was more obvious in the glulam, so the compression failure at the top

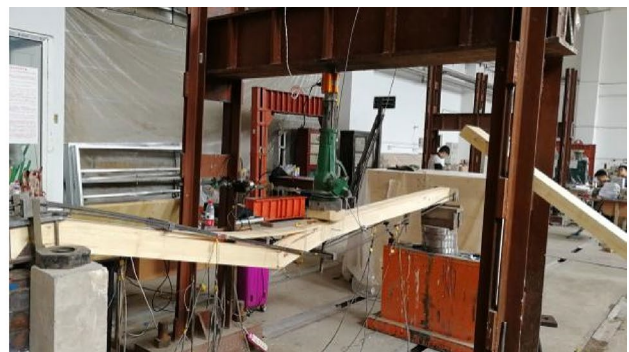
Fig. 6 Compression failure of the beam top

Fig. 7 Tension failure of the weak areas between laminates

Mei *et al. J Wood Sci*   (2021) 67:48

Page 7 of 14

Fig. 8 Instability failure

Table 3 Failure modes of specimens

Control range	Beam code	Failure mode
0	L01	Compression
	L02	Compression
18%	L11	Compression
	L12	Compression
24%	L21	Instability
	L22	Compression
30%	L31	Compression
	L32	Tension
36%	L41	Tension
	L42	Compression
42%	L51	Tension
	L52	Instability

Table 4 Ultimate load of specimens

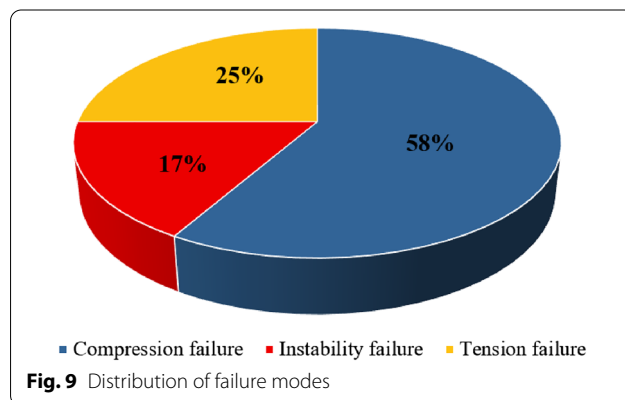| Control range (%)	Beam code	Ultimate load (kN)	Average (kN)	Increased ratio (%)
0	L01	29.15	30.08	–
	L02	31.01		
18	L11	33.02	34.17	13.60
	L12	35.32		
24	L21	40.44	40.77	35.54
	L22	41.10		
30	L31	45.42	44.04	46.41
	L32	42.66		
36	L41	44.23	43.19	43.58
	L42	42.15		
42	L51	44.70	43.65	45.11
	L52	42.60		

Fig. 9 Distribution of failure modes

of the glulam was more likely to occur. When the control range was large, the tensile stress of the steel wires and the compressive stress of the corresponding glulam part was also enormous. At this point, in the part of the glulam, the pressure generated by the beam end compressed was more significantly higher than the stress caused by

the bending moment, so its failure mode was characterized by eccentric compression members with the minor bending moment, such as out-of-plane instability, laminate tearing (similar to compression splitting), etc.

Ultimate load

As shown in Table 4 and Fig. 10, compared with the beams without prestressed control, the ultimate load of the prestressed beams increased between13.60% and 45.11%. Before the control range value reached 30%, the ultimate load of the beams rose linearly with the increase of the control range. After reaching 30%, the peak load basically remained stable due to the compressive strength of the glulam part had been fully used when the control range value was 30%. On this basis, if the control range continues to increase, the glulam part may occur out-of-plane instability or laminate tearing failure due to the excessive compressive stress, which limits the further improvement of bearing capacity. Overall, it demonstrates that there is a reasonable range of prestressed

Mei *et al. J Wood Sci*   (2021) 67:48

Page 8 of 14

Fig. 10 Tendency graph of ultimate load
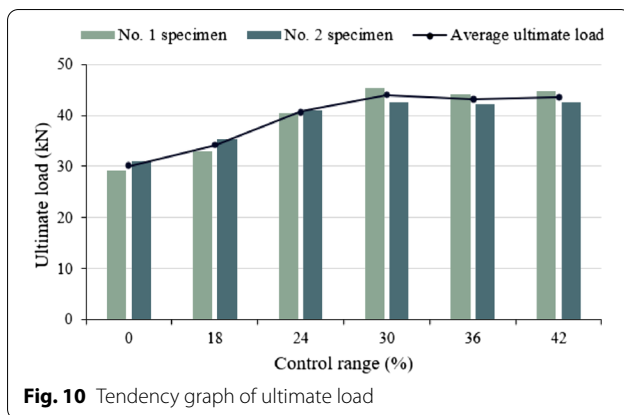
control, not the higher the control range, the better the effect.

Load–deflection relationships

Among the two beams of each group under the same working conditions, a representative one was chosen to show the load–deflection behavior, as shown in Fig. 11.

From the results plotted in Fig. 11, it can be observed that the curves of the left and right spans of the prestressed control beams were slightly different, but the general trend was the same. On the one hand, from the initial stage of loading to the final failure, with the increase of the control range, the slope of the curve and the ultimate load showed a rising trend, namely, enhancing the control range value can effectively improve stiffness and the peak load of the beams. On the other hand, the ultimate deflection decreased as the control range increased, which due to the deformation capacity of the prestressed glulam beams mainly depended on the compression yield of the glulam. When the control range was large, the beams often occurred out-of-plane instability and laminate tearing failure, so the ultimate deflection
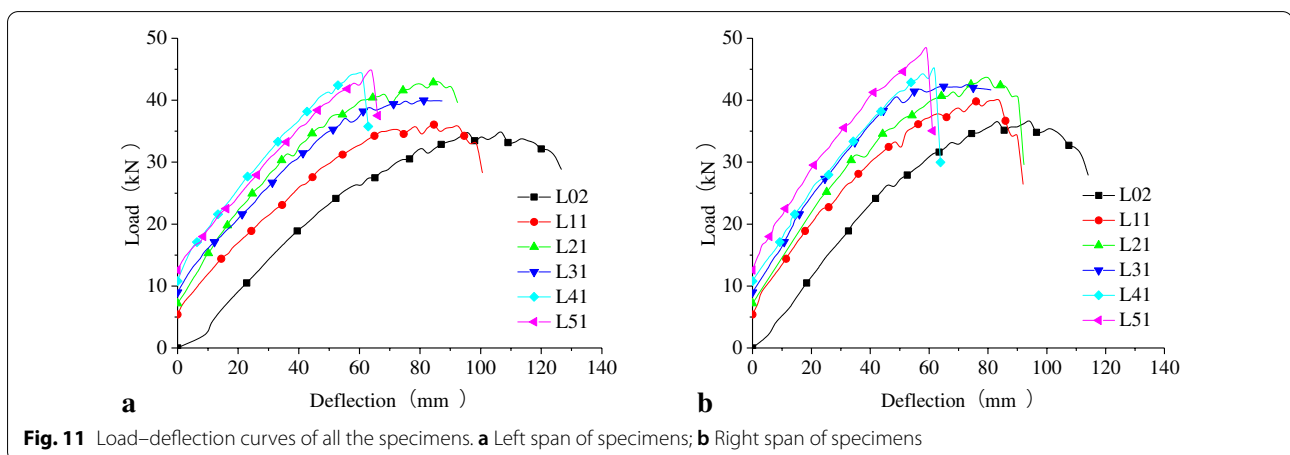
decreased. Even so, the ultimate deflection of the beams after control was still more than 1/50 of the span. By referring to the management of other structures on the ultimate deflection of the beams, the prestressed glulam continuous beam after control can still meet the design requirements.

Stress at the failure of prestressed steel wires

To study the prestressed steel wire stress under the ultimate load, experimental results are tabulated in Table 5 and plotted in Fig. 12. It can be found that the stress of the prestressed steel wires raised as the control range increased when the specimens failed. When the control range value increased to 42%, the average value of steel wires' failure stress reached 94% of the design value of tensile strength f_{py}, indicating that the steel wire strength had been effectively used.

Table 5 Failure stress of steel wires

Control range (%)	Beam code	Stress (N/mm²)	
		Test value	**Average**
0	L01	798.2	772.6
	L02	747.0	
18	L11	911.8	908.4
	L12	904.9	
24	L21	897.9	872.4
	L22	846.9	
30	L31	974.4	964.0
	L32	953.7	
36	L41	953.4	976.2
	L42	999.0	
42	L51	1063	1031
	L52	999.4	

Fig. 11 Load–deflection curves of all the specimens. **a** Left span of specimens; **b** Right span of specimens

Mei *et al. J Wood Sci*   (2021) 67:48
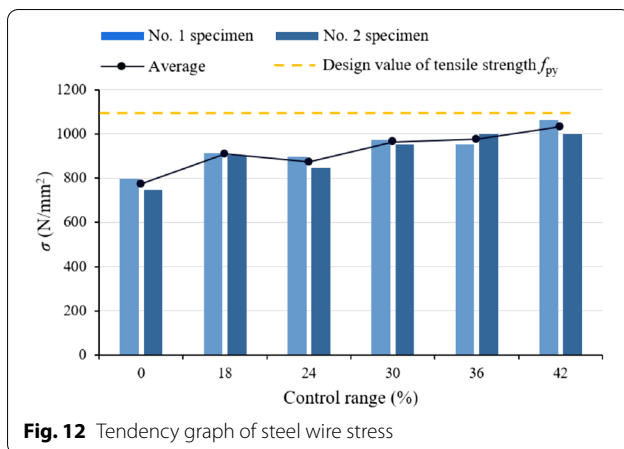
Page 9 of 14

Fig. 12 Tendency graph of steel wire stress

Besides, compared with other specimens, when the control range value was 24%, the stress value of the steel wires was abnormal and relatively low. The reason is that L21 occurred the instability failure at the loading position of the right span beam and L22 had the large wood knot at the laminate, which led to the unconventional material failure, and the material strength was not fully used. Therefore, the stress of the steel wires was abnormal when the control range value was 24%.

Load–strain relationships

Typical load–strain curves are illustrated in Fig. 13, in which 1–5 represents laminates numbers (see Fig. 14). And the negative X-axis indicates that the material is under compression; the positive X-axis demonstrates that the material is under tension; the Y-axis represents the load; the different curves show the mechanical behavior of the laminate and wire.

As the prestress control range grew, the tensile stress of the steel wires was raised, the neutral axis of the glulam section moved down, and the compressive zone enlarged. Moreover, due to the compressive part of the glulam increased gradually, its strain development of the glulam tended to be slow with the increase of the load, and the strain distribution was more uniform. It is evident that the prestress control can make the internal force redistribution of the glulam (Fig. 15), thus achieved make full use of the material properties and improve the bearing capacity of the beams.

Finite element analysis

To further study the mechanical performance of the beams with more control range values and give a reasonable range of prestressing control, a 3D finite element (FE) model was established using ABAQUS (engineering analysis software, version 6.14) to simulate the prestressed glulam continuous beams with different control range values.

Finite element model

The prestressed glulam continuous beam was composed of glulam, steel wires, and steel components. To avoid the influence of irregular mesh generation on the analysis, thus the regular simplified model was used for each element. The prestressed steel wires were defined as lines, and other components were defined as solid elements. The FE model is shown in Fig. 16.

Three steps were set up in this model, namely the initial step, prestressed control, and concentrated force. In the initial step, the constraints and boundary conditions of each component were created. The specific operation method is as follows: reference points were set at the top position of the middle of each span of the continuous beam, the reference points and the top cushion blocks of the mid-span beam were constrained by coupling. Similarly, reference points were set at the beam supports, constrained coupling with the support cushion blocks. The steel components and the glulam connecting parts were constrained by tying. Prestressing control used bolt load to offset the deflection caused by the initial load. Applying a downward concentrated force to the middle of each span of the continuous beam, the magnitude of the force was the specimens' peak load of each group. All the components (except steel wires) were meshed separately using C3D8 elements. The steel wires were meshed by the B31 elements.

Constitutive model of materials

The deformation of the steel components was considered in the design; as the stiffness of the steel components met the requirements, the elastic deformation of the steel components was not considered in the FEA, and its elastic modulus was 2.0×10^5 N/mm². According to the material testing, the elastic modulus of the prestressed steel wires was 1.92×10^5 N/mm². The behavior of glulam as an orthotropic material within the elastic range is expressed by

$$\sigma_i = D_{ij}\varepsilon_j \quad \forall \quad i,j \in \{1, 2, \ldots, 6\}, \tag{1}$$

where ε_j is the strain vector, σ_i the stress vector, and D_{ij} the stiffness matrix of the orthotropic material, as shown in Table 6.

Reasonable control range

To validate the model for the prestressed glulam continuous beam, the FE models were compared with the experimental results in this study. Owing to the limited space of this paper, only the load–deflection curves of some beams are shown in Fig. 17.
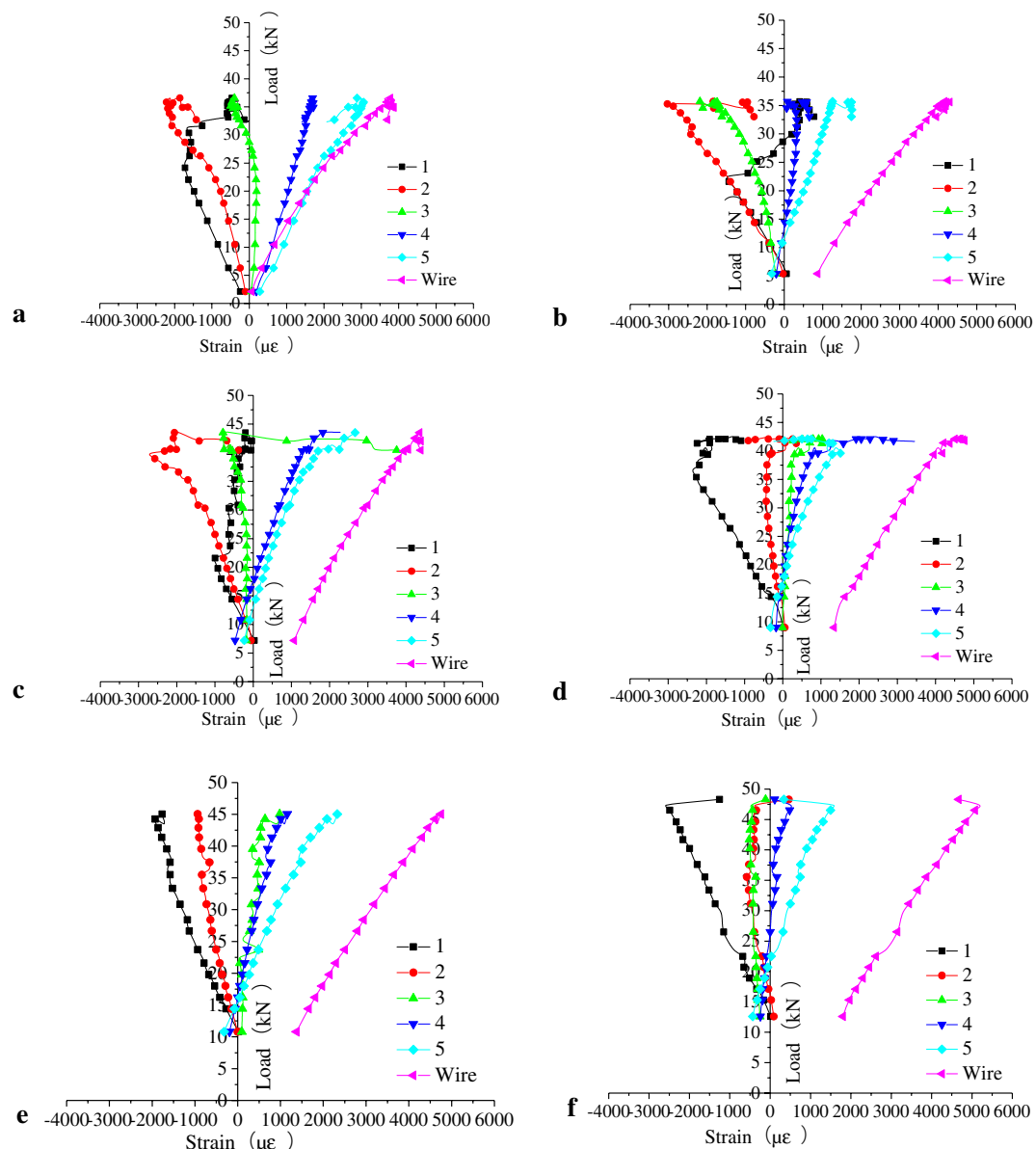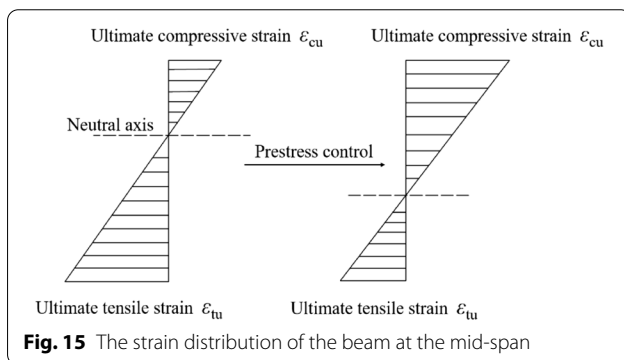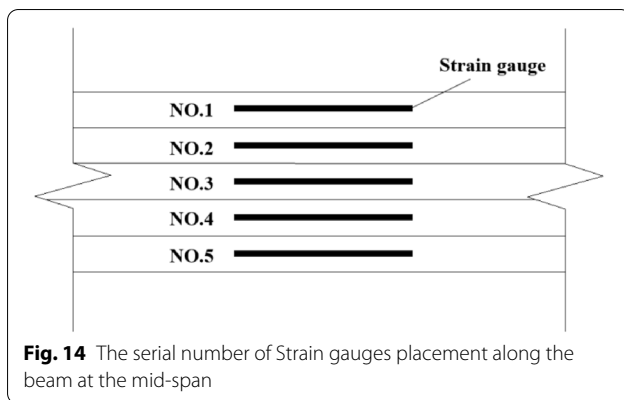
Mei *et al. J Wood Sci* (2021) 67:48

Page 10 of 14

Fig. 13 Load–strain curves of all the specimens. **a** Control 0%; **b** Control 18%; **c** Control 24%; **d** Control 30%; **e** Control 36%; **f** Control 42%

It can be concluded from Fig. 17 that the maximum error between the FE models and the experimental results was 37.6%, which indicates that the models can simulate and analyze the beams more accurately, so the control range values can be expanded through the ABAQUS. To study the reasonable range of prestressed control and compare with the results of the specimens, 6% and 12% of the control range value were added in the FEA. The specific grouping and the FEA results are shown in Table 7. Because of the limited space of this paper, to present the stress distribution of the glulam beam clearly, one span

of the continuous beam (control range value is 12%) was selected in Fig. 18. On the left side of the figure is the end of the continuous beam, and the right side of the figure is the part of the glulam beam inserted into the connection apparatus, and Fig. 18 shows the distribution of compressive stress and tensile stress parallel to grain of the beam. Due to the support at the connection, an upward support reaction force was generated. According to the deformation geometric compatibility equations and the equilibrium conditions, the bending moment distribution of the continuous beam was obtained by theoretical calculation

Fig. 14 The serial number of Strain gauges placement along the beam at the mid-span

Fig. 15 The strain distribution of the beam at the mid-span

as shown in Fig. 19. It can be seen that the top of the beam at the connection bore high tensile stress, which was the same as the simulation result.

Furthermore, the connection apparatus in Fig. 1a was made of steel, and its elastic modulus is higher than that

of glulam, which means that the steel connection apparatus had the greater stiffness and can withstand the higher load. Although the middle support of the continuous beam was subjected to large tensile stress during the loading process, which was mainly carried by the steel, and the stress shared to the end of the glulam beam was relatively small. Meanwhile, according to the experimental phenomena and results, it can be known that the final failure of the continuous beam was caused by the mid-span region. Therefore, it can be proved that the connection joint in this test can bear large tensile stress and avoid failure from occurring at the joint.

Stress of steel wires
As shown in Table 7, when the prestressed control was completed and the beam was damaged, the stress of steel wires of all beams was higher than the test results, the maximum deviation was about 17.5%. It is caused by uncontrollable factors in the test process, including different defects of glulam and uneven force applied by researchers during loading. In the FEA, glulam was an ideal material without defects, the material was fully used, so the simulation values were higher than the experimental values (Fig. 20).

Ultimate load
As illustrated in Table 7, the ultimate load of the beams can be significantly increased by prestressing control. As the control range value of the beams changed from 6 to 42%, the ultimate bearing capacity of the beam was increased by 8.86%–45.74%. A comparison between FEA and test results of the ultimate load is plotted in Fig. 21, the development trend of the curves was approximately the same, which indicates that the FEA results were relatively
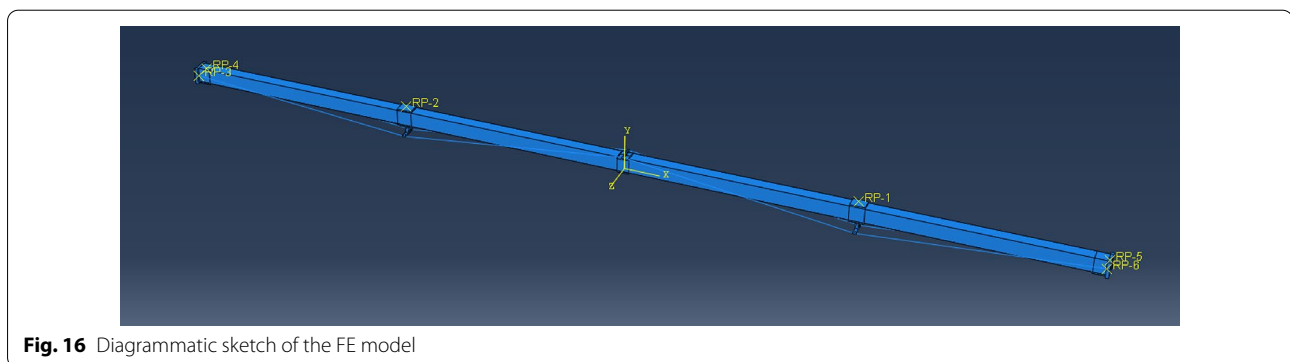

Fig. 16 Diagrammatic sketch of the FE model

Table 6 Parameters in stiffness matrix of the glulam (Unit: N/mm^2)

D_{11}	D_{22}	D_{33}	D_{44}	D_{55}	D_{66}	G_{12}	G_{13}	G_{23}
9.118×10^3	3.443×10^2	3.406×10^2	4.981×10^2	4.981×10^2	1.494×10^2	1.905×10^2	2.420×10^2	2.006×10^2

Mei *et al. J Wood Sci* (2021) 67:48

Page 12 of 14

Fig. 17 Comparison of FEA and test results. **a** Control 18%; **b** Control 30%
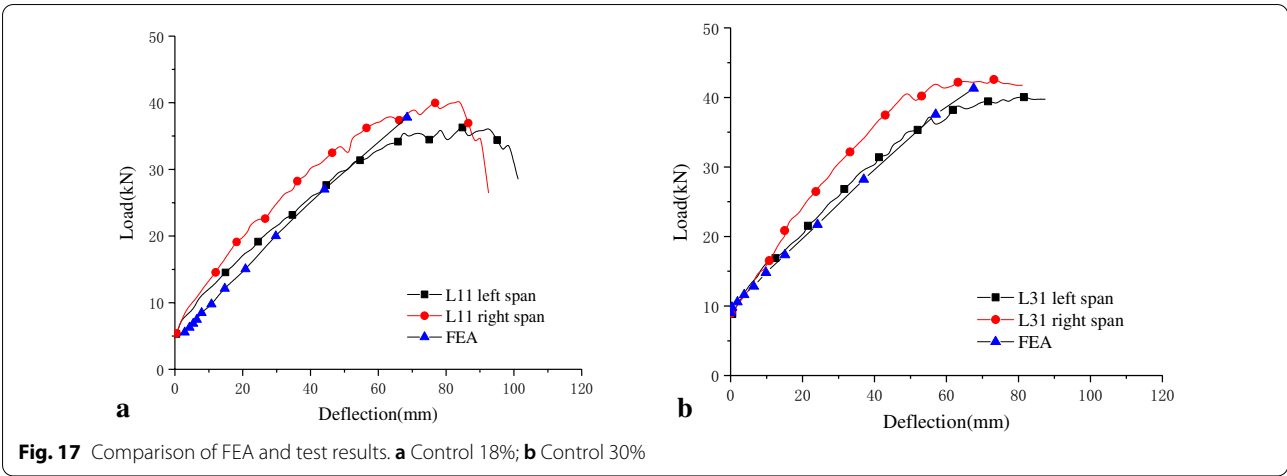
Table 7 FEA results

Beam code	Control range (%)	Continuous beam		Steel wires	
		Ultimate load (kN)	Increased ratio (%)	Control stress[a] (N/mm²)	Failure stress (N/mm²)
SL1	0	28.90	–	0	850.0
SL2	6	31.46	8.860	73.00	902.0
SL3	12	34.51	19.41	159.0	950.0
SL4	18	37.25	28.89	251.0	985.0
SL5	24	40.82	41.24	332.0	1025
SL6	30	42.12	45.74	414.0	1060
SL7	36	40.26	39.31	473.0	1085
SL8	42	38.35	32.70	555.0	1105

[a] The stress of the steel wires when the prestressed control is completed

consistent with the test results. However, when the control range increased from 36 to 42%, the ultimate load of the test beams basically remained unchanged, which was slightly different from the FEA results. That is because the control range values were high, out-of-plane instability and laminate tearing occurred in the test beams.

Furthermore, when the control range was small, the compressive stress of the beam top cannot reach the compressive strength of the glulam, the stress of steel wires and glulam increased, thus the ultimate load of the beams was improved. As the control range expanded to a certain value, the compressive stress at the top of the beam arrived at the compressive strength of the materials, and its bearing capacity was decreased. Combined with the test results and FEA, when the control range value was less than 18%, the steel wire strength was not fully used and the bearing capacity of the beam was limited. When the control range value was more than 30%, the bearing capacity of the beam would not be increased. Therefore, the reasonable control range of the prestressed glulam continuous beam was about 18%–30% of the ultimate load.
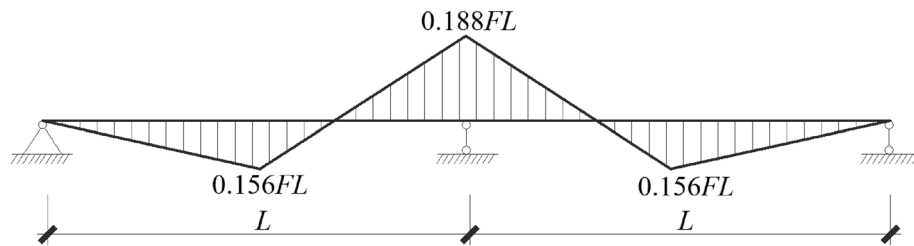

Fig. 18 Diagrammatic sketch of the stress distribution
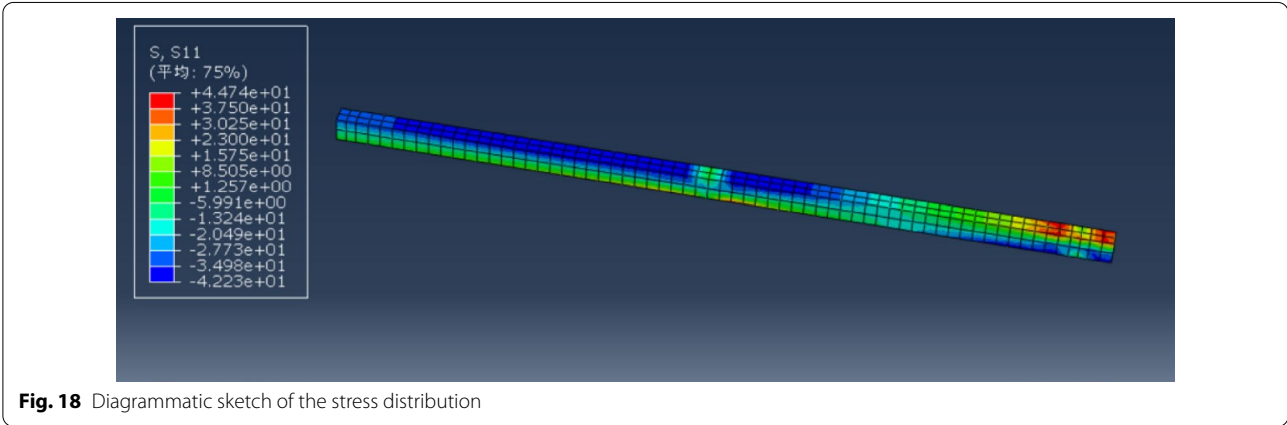
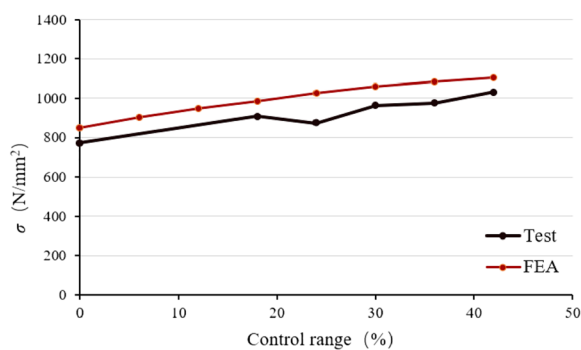**Fig. 19** Moment distribution of the continuous beam

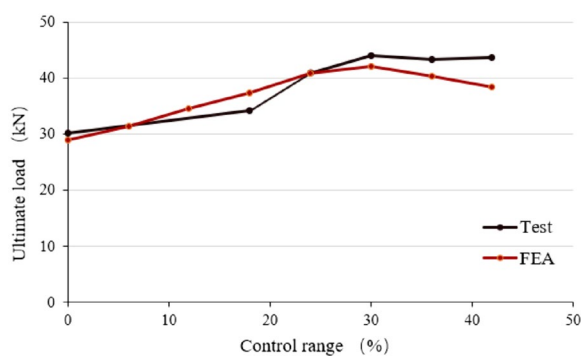**Fig. 20** Comparison between FEA and test results of the steel wire stress

Fig. 21 Comparison between FEA and test results of the ultimate load

mainly occurred compression failure. Increasing the control range, the possibility of instability failure and laminate tearing failure increased.

2. Before the control range value reached 30%, the ultimate load of the beam increased linearly as the control range increased. After that reached 30%, the ultimate load basically remained unchanged.

3. The stress of prestressed steel wires was raised with the increase of the control range. The control range value grown up from 0 to 42%, stress at the failure of the prestressed steel wires reached 94% of the design value of tensile strength f_{py}, which demonstrates that the strength of steel wire had been fully used.

4. Based on the test and FEA results, the control range value was low than 18%, the bearing capacity of the beam was limited, and the steel wire strength was not fully used. When the control range value was more than 30%, the bearing capacity of the beam would not be increased. Therefore, the reasonable control range of the prestressed glulam continuous beams was about 18%–30% of its estimated ultimate load.

Conclusions

1. For the prestressed glulam continuous beams, there were three main failure modes, which were compression failure at the top of the beam, tension failure of the weak areas between laminates, and instability failure. The probability of three kinds of failure was 58%, 25% and 17%, respectively. When the control range was small, the glulam continuous beams

Authors' contributions
LM wrote the draft of this manuscript. NG formulated and designed the experiments. LL and HZ analyzed the data. YZ reviewed and edited the manuscript. All authors read and approved the final manuscript.

Availability of data and materials
The datasets used and/or analyzed during the current study are available from the corresponding author on reasonable request.

Mei *et al. J Wood Sci*   (2021) 67:48

Page 14 of 14

Declarations

Author details
[1]College of Civil Engineering, Northeast Forestry University, Harbin 150040, China. [2]College of Civil Engineering and Architecture, Wuyi University, Wuyishan 354300, China.

References
1. Elnaklah R, Walker I, Natarajan S (2021) Moving to a green building: Indoor environment quality, thermal comfort and health. Build ment 191:107592
2. He M, Luo J, Tao D, Li Z, Sun YL, He GR (2020) Rotational behavior of bolted glulam beam-to-column connections with knee brace. Eng Struct 207:110251
3. Issa CA, Kmeid Z (2005) Advanced wood engineering: glulam beams. Constr Build Mater 19(2):99–106
4. Song JW, Chen CJ, Zhu SZ, Zhu MW, Dai JQ, Ray U, Li YJ, Kuang YD, Li YF, Quispe N, Yao YG, Gong A, Leiste UH, Bruck HA, Zhu JY, Vellore A, Li H, Minus ML, Jia Z, Martini A, Li T, Hu LB (2018) Processing bulk natural wood into a high-performance structural material. Nature 554(7691):224–228
5. Zuo HL, Di J, Wang T, Guo N (2019) Lateral performance of prestressed diagonal cross-bar reinforced timber shear walls under cyclic loading. J Northeast For Univ 47(06):61–64. https://doi.org/10.13759/j.cnki.dlxb.2019.06.012 (**in Chinese**)
6. Mei LD, Guo N, Zuo HL, Li L, Li GD (2021) Influence of the force arm on the flexural performance of prestressed glulam beams. Adv Civil Eng 2021:1–16
7. Tazarv M, Carnahan Z, Wehbe N (2019) Glulam timber bridges for local roads. Eng Struct 188:11–23
8. Buchanan AH, Fairweather RH (1993) Seismic design of glulam structures. Bull N Z Soc Earthq Eng 26(4):415–436
9. Ehrhart T, Steiger R, Palma P, Gehri E, Frangi A (2020) Glulam columns made of European beech timber: compressive strength and stiffness parallel to the grain, buckling resistance and adaptation of the effective-length method according to Eurocode 5. Mater Struct 53(4):1–12
10. Zuo HL, Li YS, Fu DQ, Guo N (2019) Bending performance test on the different forms of reinforced glulam beams. J Northeast For Univ 47(08):62–65. https://doi.org/10.13759/j.cnki.dlxb.2019.08.012 (**in Chinese**)
11. Yang YL, Liu JW, Xiong GJ (2013) Flexural behavior of wood beams strengthened with HFRP. Constr Build Mater 43:118–124
12. Zhang J, Wang WC, Qiu RG, Shen H, Xu QF, Gao S (2019) Experimental study on short-term flexural behavior of internal prestressed glulam beams. Chin Soc Civil Eng 52(05):23–34
13. Yang HF, Liu WQ, Lu WD, Zhu SJ, Geng QF (2016) Flexural behavior of FRP and steel reinforced glulam beams: experimental and theoretical evaluation. Constr Build Mater 106:550–563
14. Dolan CW, Galloway TL, Tsunemori A (1997) Prestressed glued-laminated timber beam—Pilot study. J Compos Constr 1(1):10–16
15. Frese M, Blass HJ (2009) Bending strength of spruce glulam. Eur J Wood Wood Prod 67(3):277–286
16. Frese M, Enders-Comberg M, Blass HJ, Glos P (2012) Compressive strength of spruce glulam. Eur J Wood Wood Prod 70(6):801–809
17. De Lorenzis L, Scialpi V, La Tegola A (2005) Analytical and experimental Study on bonded-in CFRP bars in glulam timber. Compos B Eng 36(4):279–289
18. Liu W, Yang HF (2008) Experimental study on flexural behavior of engineering wood beams. J Build Struct 29(01):90–95
19. De Luca V, Marano C (2011) Prestressed glulam timbers reinforced with steel bars. Constr Build Mater 30:206–217
20. Guo N, Wang YJ, Zuo HL (2017) Study of short-term flexural behavior for glue-bamboo and lumber beams under different pre-stressed states. Civil Eng J. https://doi.org/10.14311/CEJ.2017.02.0012
21. Guo N, Wang WB, Zuo HL (2019) flexural property of string beam of pre-stressed glulam based on influence of regulation and control. SDHM Struct Durabil Health Monit 13(2):143–179
22. Uzel M, Togay A, Anil O, Sogutlu C (2018) Experimental investigation of flexural behavior of glulam beams reinforced with different bonding surface materials. Constr Build Mater 158:149–163
23. Ribeiro AS, De Jesus AMP, Lima AM, Lousada JLC (2009) Study of strengthening solutions for glued-laminated wood beams of maritime pine wood. Constr Build Mater 23(8):2738–2745
24. Zuo HL, Liu HR, Lu JX (2020) Effect of new self-tapping screw reinforcement measures on bending performance of glulam beams. J Northeast For Univ. 48 (05): 112–116 + 121. https://doi.org/10.13759/j.cnki.dlxb.2020.05.022. (**in Chinese**).
25. Yang XH, Xue W, Guo N (2017) Bending performance of glued-lumber beam reinforced with steel plate. J Jilin Univ Eng Technol Ed 2:468–477. https://doi.org/10.13229/j.cnki.jdxbgxb201702017
26. Anshari B, Guan ZW, Kitamori A, Jung K, Komatsu K (2012) Structural behaviour of glued laminated timber beams pre-stressed by compressed wood. Constr Build Mater 29(4):24–32
27. Yang HF, Ju DD, Liu WQ, Lu WD (2016) Prestressed glulam beams reinforced with CFRP bars. Constr Build Mater 109:73–83
28. McConnell E, McPolin D, Taylor S (2014) Post-tensioning of glulam timber with steel tendons. Constr Build Mater 73:426–433
29. Yang YW (2015) The study on flexural performance of prestressed glulam beams string structure based on the creep behavior. Chinese master's thesis, Northeast For Univ. https://kns.cnki.net/kcms/detail/detail.aspx?dbcode=CMFD&dbname=CMFD201601&filename=1015655642.nh&v=umz5iBe1PfFwRCZQqa%25mmd2FZ2fz5Og%25mmd2F8dPamyLAQOFNmCm%25mmd2Fb4FLbbixMucfer3dMxqhc (**in Chinese**)
30. GB, T 50329-2012 (2012) Wood construction design standard. China Architecture & Building Press, Beijing
31. GB, T 228.1-2010 (2010) Metallic materials-tensile testing-part 1: method of test at room temperature. Standards Press of China, Beijing
32. GB, T 50152-2012 (2012) Standard for test method of concrete structures. China Archi-tecture & Building Press, Beijing